

NRL Report 6080

Optical Tests on Some Ruby Samples

J. N. BRADFORD, R. C. ECKARDT, AND J. W. TUCKER

*Radiometry Branch
Optics Division*

March 6, 1964



U.S. NAVAL RESEARCH LABORATORY
Washington, D.C.

CONTENTS

Abstract	ii
Problem Status	ii
Authorization	ii
INTRODUCTION	1
TESTS PERFORMED	2
OPTIC AXIS FIGURES - GENERAL	2
Uniaxial Crystals	2
Biaxial Crystals	4
EFFECT OF AXIS VARIATIONS	4
OPTIC AXIS FIGURES OF RUBY SAMPLES	4
Airtron (Flux-Grown)	4
Linde 1739-18	5
Linde 1830-16	5
Thermal Syndicate 636	5
Thermal Syndicate 621	8
SHADOWGRAPHS	8
SMALL-ANGLE SCATTERING	15
GENERAL OBSERVATIONS	22
FUTURE TESTS	22

Copies available at Office of Technical Services
 Department of Commerce - \$.75

ABSTRACT

Six samples of ruby crystals grown by the Linde Company, Thermal Syndicate, Ltd., and Airtron have been subjected to several optical tests. The four types of tests performed are based on optic axis figure, shadowgraphs, examination between crossed polarizers, and small-angle scattering. The test results are presented primarily in photographic form.

Optic axis figures were reasonably good in all but one of the samples examined. The shadowgraphs show striae in all of the samples and in some, wedges resulting from relatively uniform refractive-index gradients. One sample shows no small-angle scattering. In the other samples small-angle scattering is quite variable and strongly dependent on direction of transmission through the crystals. Examination between crossed polarizers provided no additional information.

It is expected that facilities will soon be available for interferometric and spectroscopic studies and evaluations of ruby.

PROBLEM STATUS

This is an interim report on one phase of the problem; work is continuing on another phase.

AUTHORIZATION

NRL Problem N01-09
ARPA Order 306-62

Manuscript submitted February 20, 1964.

OPTICAL TESTS ON SOME RUBY SAMPLES

INTRODUCTION

Ruby used in the ARPA laser program has been inferior to glass in optical quality and requires substantial improvement for theoretical laser performance to be achieved. Efforts are being made by the suppliers of ruby to synthesize material of greater uniformity. The Naval Research Laboratory is helping to monitor this program by conducting tests on samples submitted through ONR. The present concern is to compare materials on a relative basis rather than to derive precise numbers, as the latter would suggest a degree of uniformity that does not exist in present materials. Numbers might be meaningful if enough material were available for a statistical analysis. This is not the case nor would there be much point in such an analysis while this far away from the ultimate goal.

The samples received have been rough cuts from boules grown by the Linde Company,* and Thermal Syndicate Ltd. and crystals of flux-grown ruby grown by Airtron** (Table 1). The samples were cut and polished as indicated in the table and are shown in their final form in Fig. 1.

Table 1
Ruby Samples Tested

Sample	Form Supplied	Form Tested
Airtron	Flux-grown crystal	Two faces perpendicular to optic axis polished flat. 5.3 mm thick.
Linde 1963-19	90° finished rod, 9.5 mm × 58.9 mm	90° finished rod, 9.5 mm diameter × 58.9 mm long.
Linde 1739-18	60° boule	Cube 8.9 mm on a side. Optic axis perpendicular to two faces.
Linde 1830-16	90° boule	Cube 10.2 mm on a side.
Thermal Syndicate 636	90° boule	Cube 10.1 mm on a side.
Thermal Syndicate 621	90° boule	Cube 6.5 mm on a side.

* Division of Union Carbide Corporation

** Division of Litton Industries

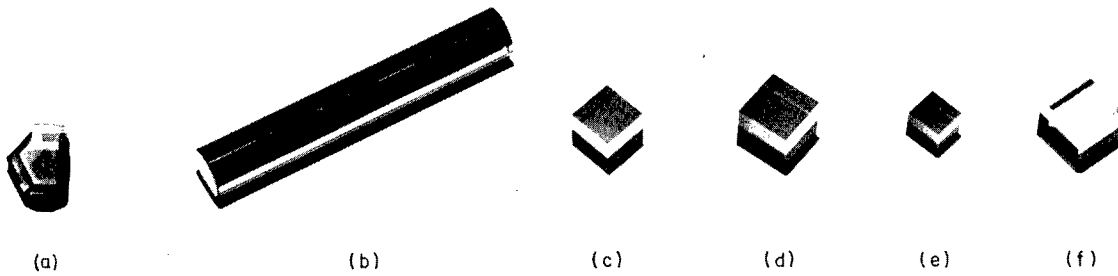


Fig. 1 - Ruby samples: (a) Airtron; (b) Linde 1963-19; (c) Linde 1739-18; (d) Linde 1830-16; (e) Thermal Syndicate 621; (f) Thermal Syndicate 636

TESTS PERFORMED

Four types of tests were made on each sample, based on optic axis figure, shadowgraphs, examination between crossed polarizers, and small-angle scattering.

The optic axis figure consists of an isogyre pattern, ideally a dark cross, and isochromates or color circles. The isogyre pattern is unique in that it is affected by a single physical characteristic of the crystal - the uniformity of direction of the optic axis. The isochromates are affected by both axis deviations and variations of optical path through the sample. Since the optic axis test examines any extensive sample bit by bit, a group of pictures is presented for each of the larger samples. In evaluating these data as well as those from the other tests, the thickness of the sample must be considered.

Shadowgraphs are pictures of the sample formed by light from a distant point source. As this light passes through the sample it projects an image of the internal structure of the ruby onto photographic film. Index aberrations cause refraction and a corresponding pattern of film illumination. Two sample-to-film distances are used so that the effects of refraction may be more readily recognized. In many of the pictures an optical wedge effect is apparent. Since this cannot be accounted for geometrically it must result from a small but relatively uniform gradient in index of refraction.

When crossed polarizers are used in the preceding optical arrangement, it might be expected that photoelastic effects would contribute additional structure detail, but additional structure data are obtained only in a direction along or nearly along the optic axis of the crystal. It seems evident that optic axis variation gives this extra structure since in this direction transmission should be very sensitive to axis direction.

The small-angle-scattering photographs give an engineering picture of what the sample does to a beam of light. Red light from a gas laser is sharply defined by a small circular aperture. After passing through the ruby sample the beam is focussed by a telescope onto photographic film. Distortion of the angular diffraction pattern of the beam gives a picture of the angular scattering introduced by the sample. Beam deviation is not indicated in the pictures but this phenomenon is clearly visible in the shadowgraphs.

OPTIC AXIS FIGURES - GENERAL

Uniaxial Crystals

Ruby is ideally a uniaxial doubly refracting crystal. Light passing through such a medium is separated into two waves, the O or ordinary wave and the E or extraordinary wave. The waves have mutually perpendicular polarization directions and travel with

different velocities. The O wave is polarized at right angles to the plane formed by the ray direction and the optic axis, the principal plane, while the E wave is polarized in the principal plane and at right angles to the ray direction. As the ray direction approaches the direction of the optic axis the velocity of the extraordinary wave approaches that of the ordinary wave, and the two waves are indistinguishable along the optic axis.

To produce an optic axis figure, the uniaxial crystal is mounted in convergent light between crossed polarizers with the optic axis along the line of sight (Fig. 2). When the incident light is polarized in the principal plane or at right angles to the principal plane,* a single wave is transmitted by the crystal, an E wave or an O wave, and this light is blocked by the second polarizer. If the principal plane is neither parallel nor perpendicular to the plane of polarization of the incident light, then the incident wave is resolved into O and E waves. Since these waves travel with different velocities, their relative phase at exit depends upon the optical path difference for the two waves. When the optical path difference is an integral number of wavelengths for light of a given wavelength, that light emerges in the state of polarization in which it enters, and the second polarizer blocks it. With white light, colors arise because of the partial subtraction of spectral regions adjacent to this wavelength.

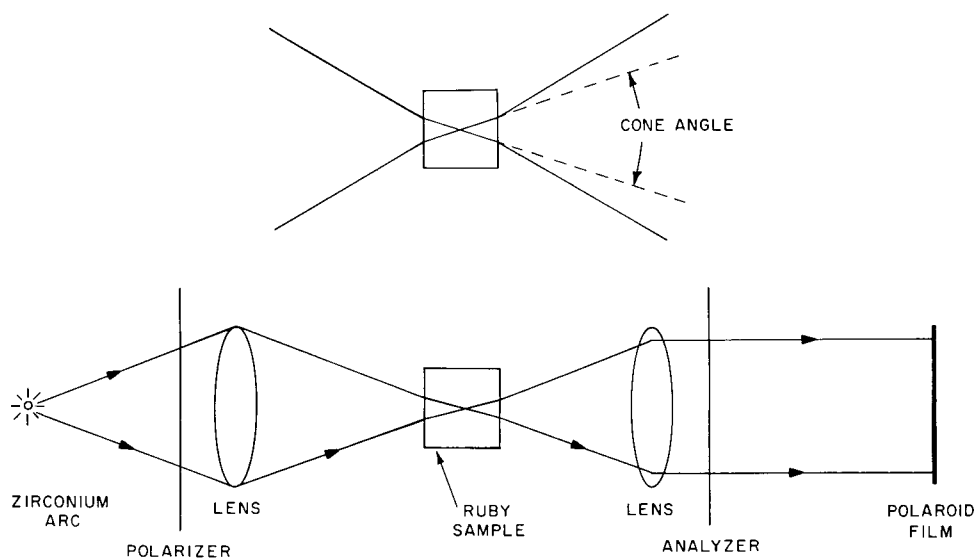


Fig. 2 - Optical system to obtain optic axis figure

Since no light gets through with principal plane parallel or perpendicular to the first polarizer, regardless of its wavelength or direction with respect to the optic axis, a prominent feature of the light pattern on the film should be a dark cross or isogyre pattern centered where rays parallel to the optic axis focus on the film and with dark arms extending in the directions of polarization of the polarizers. It should be noted that neither the location nor the general appearance of this cross is sensitive to optical path. A gross change in thickness would simply change the apparent magnification of the isogyre pattern. The symmetry of the isogyre pattern is indicative of the uniformity of direction of the optic axis in the crystal.

A second feature of the optic axis interference figure is a set of color circles or, in the case of monochromatic light, of dark circles filling the otherwise light areas. These

*Born and Wolf, "Principles of Optics," Pergamon Press, 1959, page 677

circles are loci of constant phase differences between the O and E waves. These loci are affected by variations in index of refraction and path length as well as by axis variations and for this reason they are less useful as a clue to axis uniformity.

Biaxial Crystals

A biaxial crystal in convergent light between crossed polarizers produces a figure that depends in detail on the orientation of the axial plane relative to the polarization directions. In general the isogyre pattern is a hyperbola asymptotic to the polarization directions and the isochromates are ellipses with major axes passing through the points corresponding to the optic axis directions (Fig. 3). These points are at the intersection of the major axes with the hyperbola. Ruby often exhibits an optic axis figure characteristic of a biaxial crystal with several degrees separation between the optic axes.

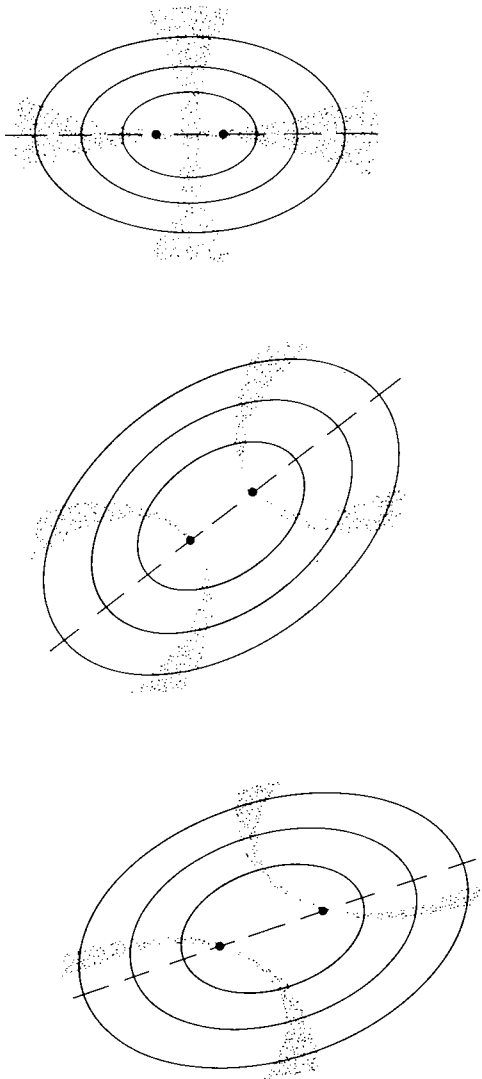


Fig. 3 - Optic axis figures of biaxial crystals

EFFECT OF AXIS VARIATIONS

If the optic axis of a uniaxial crystal has different directions in different parts of the crystal, the optic axis figure can become quite scrambled and difficult to interpret with any accuracy. In such cases it is probably enough to say that the picture indicates a substantial variation in axis direction. Where the isogyre pattern is distorted but recognizable it is often possible to estimate the magnitude of the angular deviation involved. This is a qualitative estimate based on observations of simulated patterns from tandem sections of perfect uniaxial crystal with axes slightly misaligned. That portion of the isogyre outside of the first color circle is especially sensitive to axis variations and disappears if this is more than a few degrees in a direction transverse to the isogyre. This feature distinguishes the effect of axis variation from the pattern of a biaxial crystal.

OPTIC AXIS FIGURES OF RUBY SAMPLES

Airtron (Flux-Grown)

The Airtron sample is a flux-grown crystal with several natural facets. For these tests, the two facets perpendicular to the optic axis were ground flat and optically polished. The first six optic axis pictures were made looking along the optic axis at adjacent and partially overlapping areas of the crystal (Fig. 4). The primary light source is essentially a point source and it is focussed down in the crystal so that the volume of crystal contributing to the figure is contained within a double cone. In this instance the vertex angle of the cone, and therefore the equivalent angular diameter of the

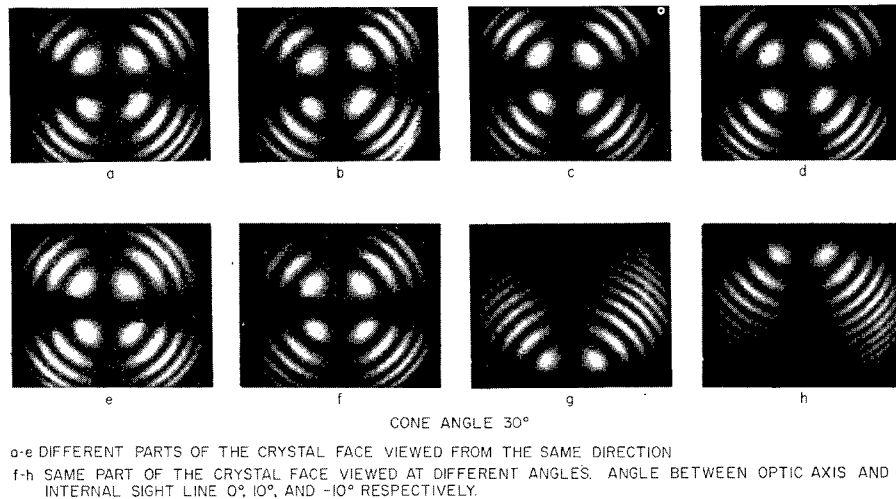


Fig. 4 - Optic axis figure of Airtron flux-grown sample

illuminated area in the figures, is 30 degrees. The last two figures show the effect of tilting the axis 10 degrees down and up from the line of sight. From the standpoint of optic axis figure this Airtron ruby is very good. There is just a suggestion of the biaxial figure (Fig. 4b and 4e). This is presumed to be due to the strain in those parts of the crystal near the edges.

Linde 1739-18

A cube with side dimension 8.9 mm was cut and polished from Linde boule 1739-18. Optic axis figures were photographed at five nominal positions on a face normal to the optic axis. Two such sets of photographs were obtained and are shown in the relative positions in which they were made (Fig. 5). From this type of layout of views (Figs. 5, 7, 8,9) and from shadowgraphs shown later in this report (Figs. 13-16), one may see where striae appeared in the regions observed. The scale is such that the diameter of the illuminated area corresponds to 24 degrees. The set of pictures in Fig. 6 was taken through the center of the cube with the cube tilted about a horizontal axis.

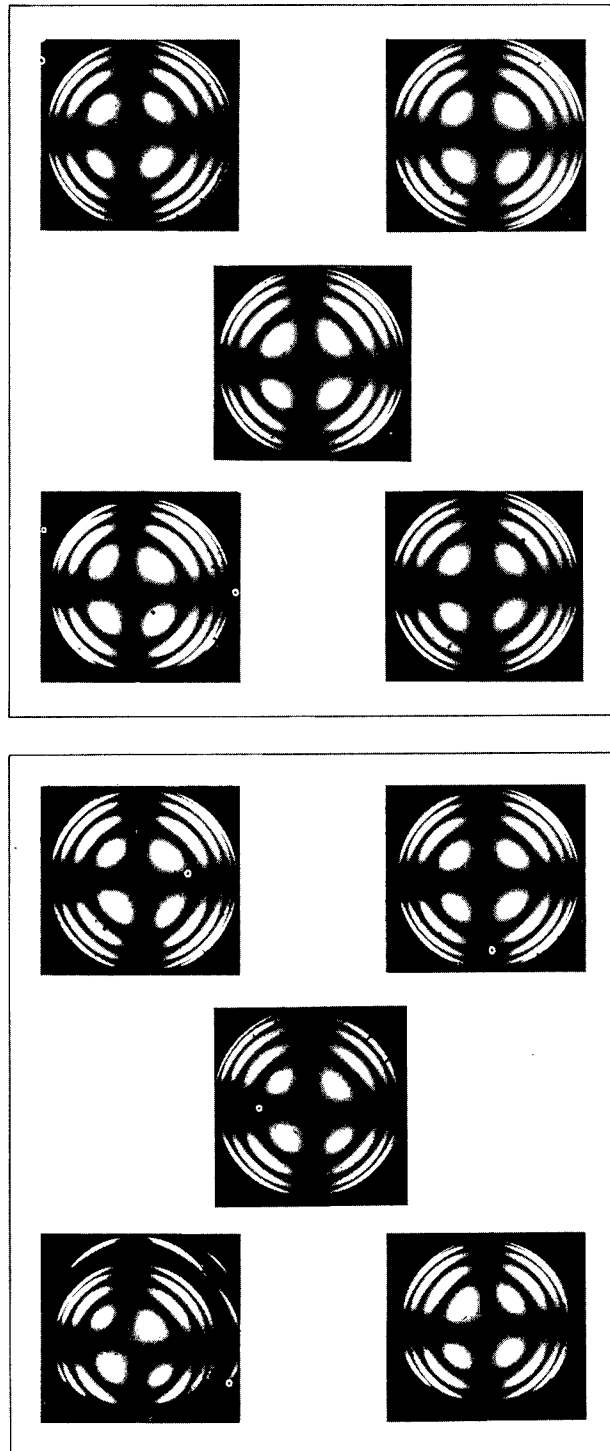
This material is seen to have good axis uniformity generally (one or two degrees) although it shows some evidence of biaxiality near the edges of the cube. The fact that equivalent pictures are not identical is due to the accidental differences in the portions of the sample irradiated even for the same nominal positions.

Linde 1830-16

A cube with side dimension 10.2 mm was cut and polished from Linde boule 1830-16. Optic axis figures were photographed at the five nominal positions over the face normal to the optic axis (Fig. 7). This material exhibits a high degree of axis uniformity (less than one degree variation) with no evidence of biaxiality.

Thermal Syndicate 636

A cube with side dimension 10.1 mm was cut and polished from Thermal Syndicate boule 636. Optic axis figures were photographed at five nominal positions over the face



CUBE EDGE 8.9mm - CONE ANGLE 24°

Fig. 5 - Optic axis figures of Linde 1739-18

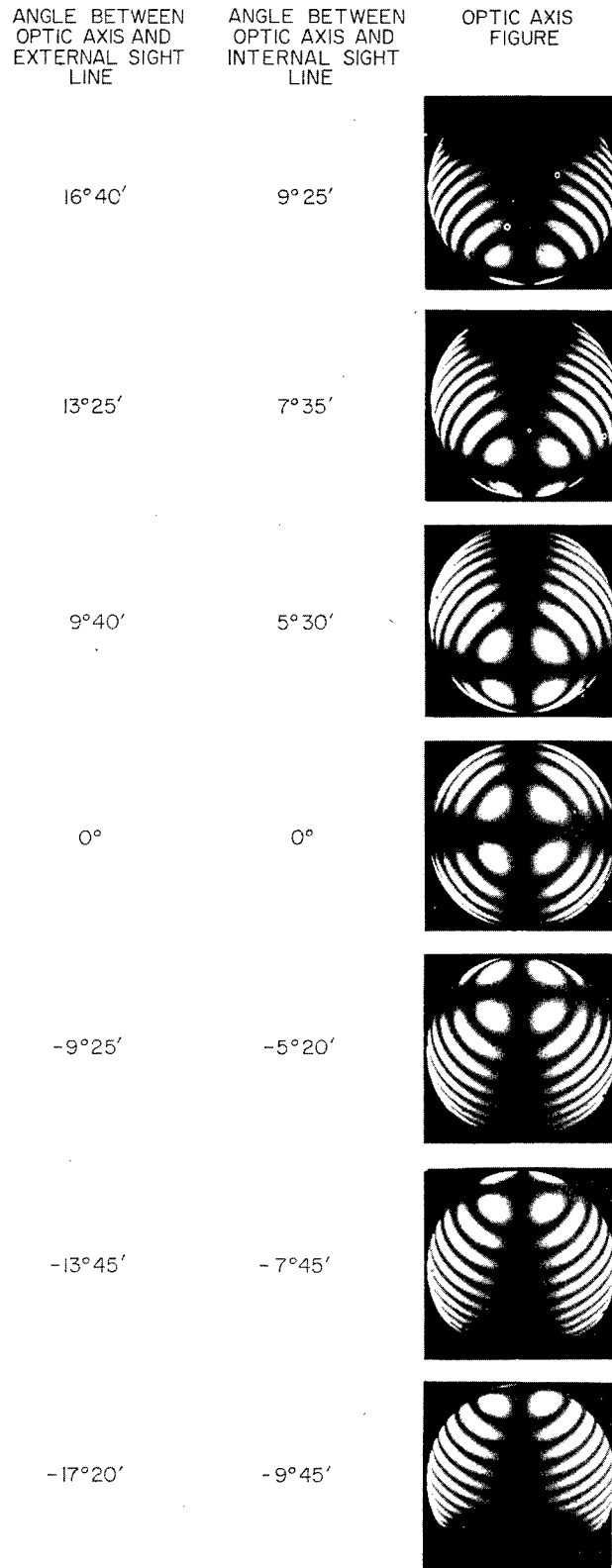
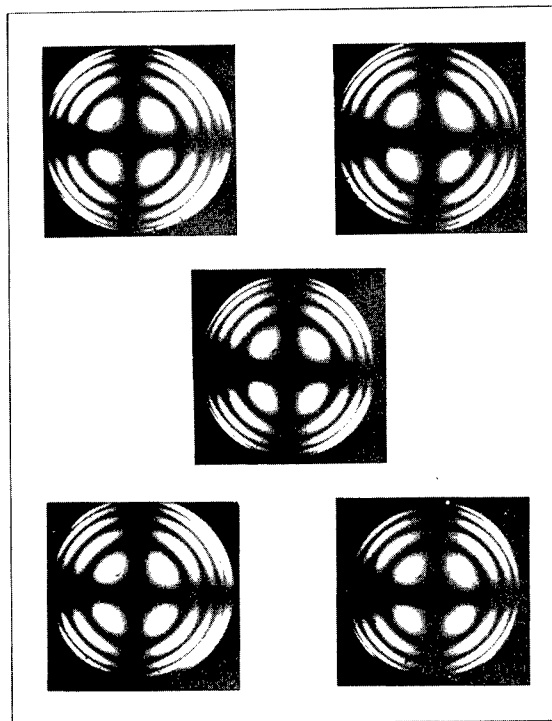


Fig. 6 - Angular variations of the optic axis figure of Linde 1739-18



CUBE EDGE 10.2mm - CONE ANGLE 24°

Fig. 7 - Optic axis figures of Linde 1830-16

normal to the optic axis (Fig. 8). These figures all indicate variation of the optic axis of at least several degrees. The distorted central cross is all that remains of the isogyre pattern and this is variable from position to position.

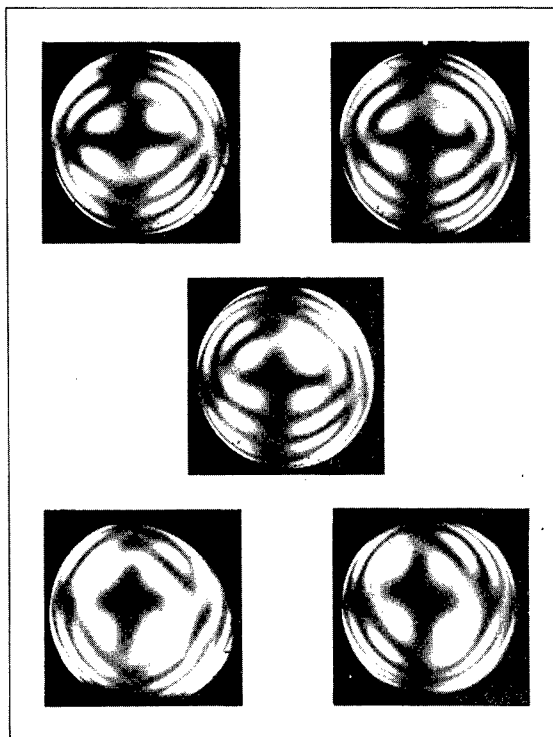
Thermal Syndicate 621

A cube with side dimension 6.5 mm was cut and polished from Thermal Syndicate boule 621. Optic axis figures were again photographed for five nominal positions over the face normal to the optic axis (Fig. 9). The partial disappearance of just the horizontal brush of the isogyre pattern indicates some axis variation in a vertical direction (one to two degrees). The color circles, isochromates, are relatively undistorted but show some anomaly at the horizontal brush. This suggests that the index of refraction is uniform except as modified by axis variations. It should be mentioned that the original boule of this material showed a very poor optic axis figure. The small size of the cube obtained from the boule was brought about by cracking of the boule during cutting. It is possible that this crack developed along a boundary separating regions of the boule with different axis directions.

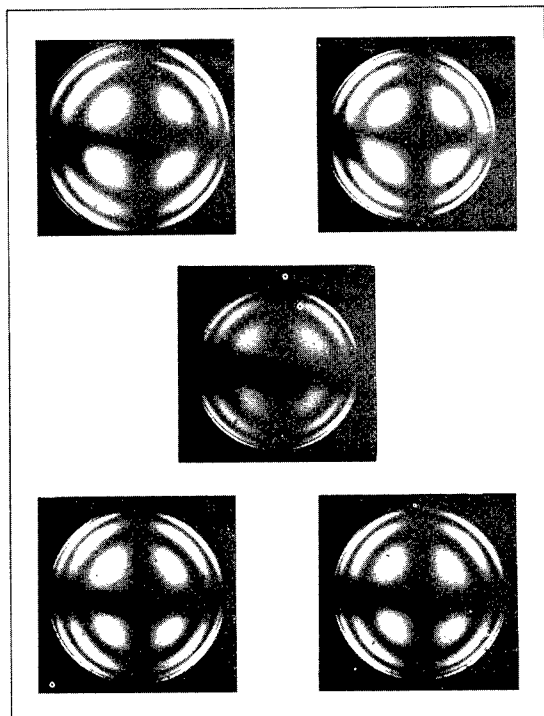
SHADOWGRAPHS

Ruby, if a good optical medium, should not scatter or otherwise disturb the angular distribution of light passing through it. The ideal is not achieved, in general, and scattering and other deviations often occur in actual crystals.

Fig. 8 - Optic axis figures of Thermal
Syndicate 636



CUBE EDGE 10.1mm - CONE ANGLE 24°



CUBE EDGE 65mm - CONE ANGLE 24°

Fig. 9 - Optic axis figures of Thermal
Syndicate 621

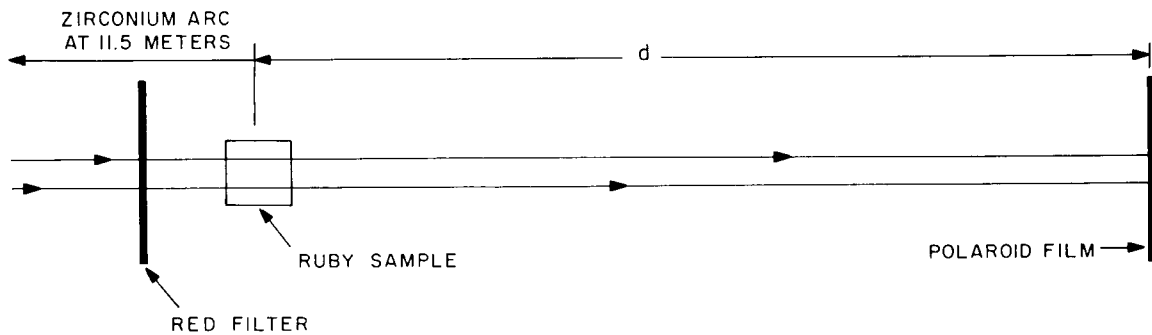


Fig. 10 - Optical system to produce shadowgraphs. Shadowgraphs were made with 1/2-second exposures on #47 Polaroid film. The red filter was used to eliminate light which would excite phosphorescence. Two sample-to-film distances were used; $d = 18$ cm and $d = 85$ cm.

Some of these deviations, notably those brought about by striae (gross non-uniformities of refractive index), may be observed readily by the shadowgraph technique. This method records on photographic film the shadow cast by a sample in light from a point source (Fig. 10). The features of interest are not truly shadows but spatial variations in illuminance on the film resulting from angular light deviations localized in the crystals.

For the photographs presented here (Figs. 11-16), the light source was a forty-watt zirconium arc about 11.5 meters from the crystals. Shadowgraphs were made at two distances from the samples, 18 cm and 85 cm, in order to give some impression of angular magnitudes. In the figures, the symbols \parallel and \perp indicate whether the incident light was parallel or perpendicular, respectively, to the optic axes. In each of the cubes two pairs of faces define transmission directions perpendicular to the optic axis and subscripts 1 and 2 are used to identify these.



Fig. 11 - Shadowgraphs of Airtron flux-grown sample: (a) film 18 cm from crystal; (b) film 85 cm from crystal



Fig. 12 - Shadowgraphs of Ruby rod, Linde 1963-19: (a) film 18 cm from crystal; (b) film 85 cm from crystal

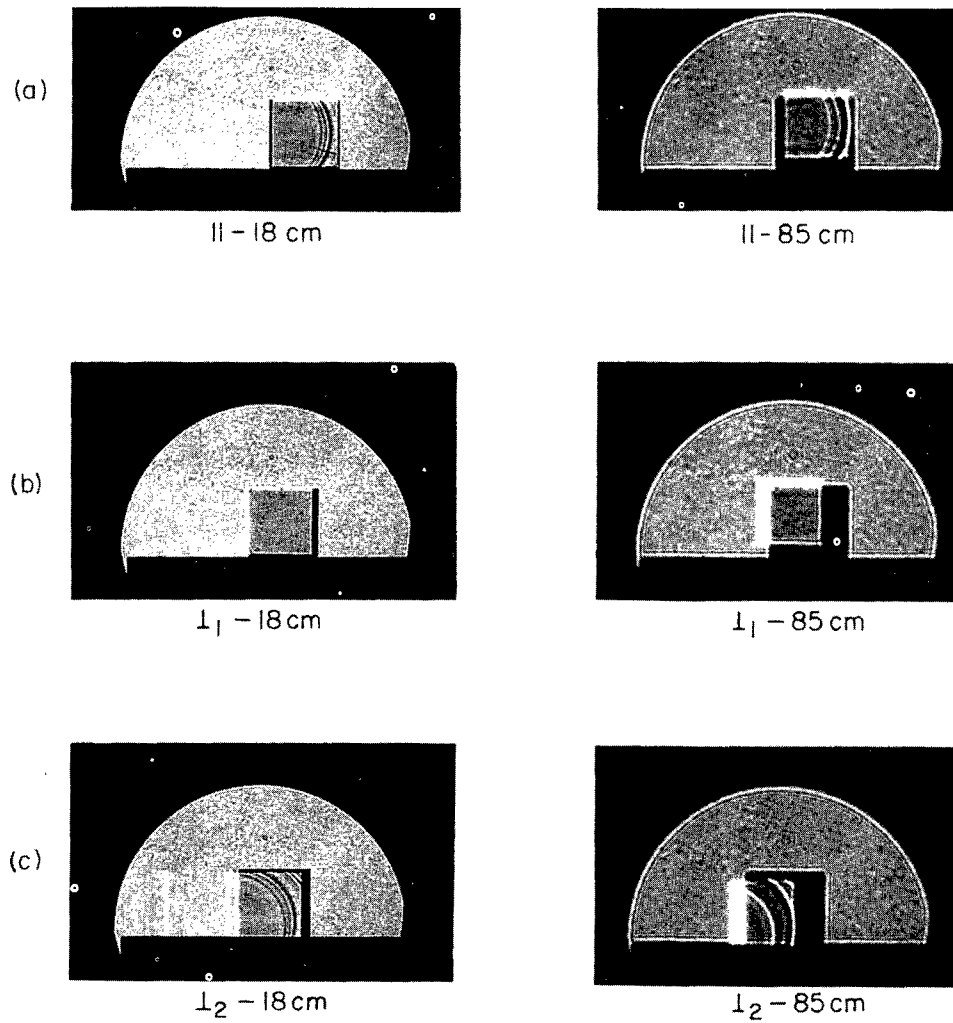


Fig. 13 - Shadowgraphs of Linde 1739-18: (a) parallel to optic axis; (b) first direction perpendicular to optic axis; (c) second direction perpendicular to optic axis

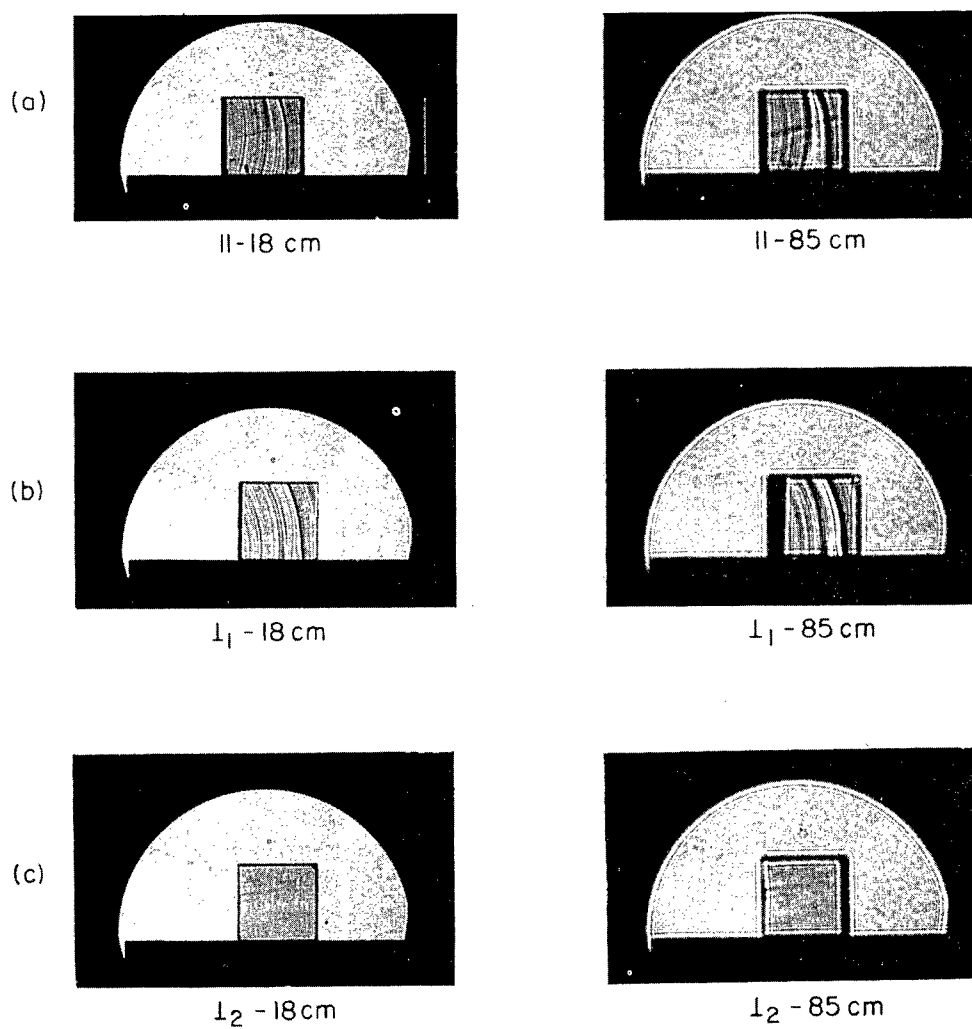


Fig. 14 - Shadowgraphs of Linde 1830-16: (a) parallel to optic axis; (b) first direction perpendicular to optic axis; (c) second direction perpendicular to optic axis

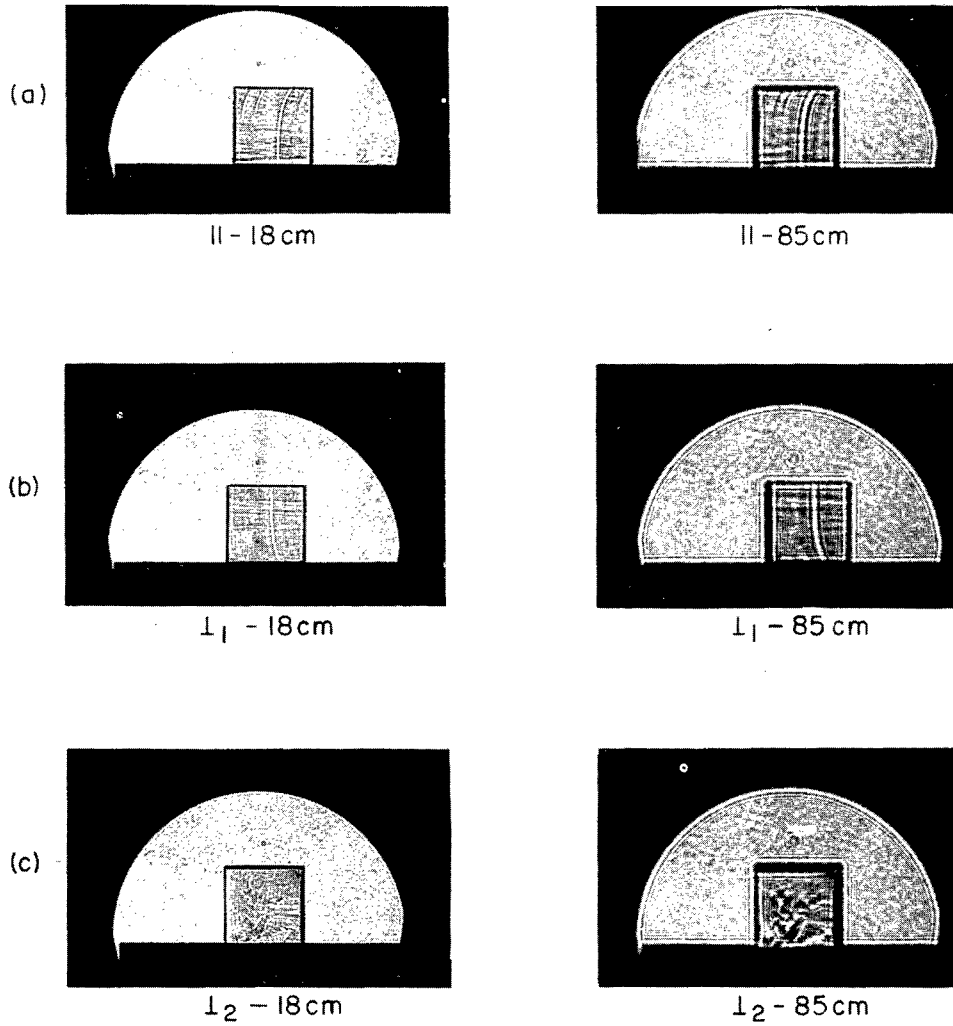


Fig. 15 - Shadowgraphs of Thermal Syndicate 636: (a) parallel to optic axis; (b) first direction perpendicular to optic axis; (c) second direction perpendicular to optic axis

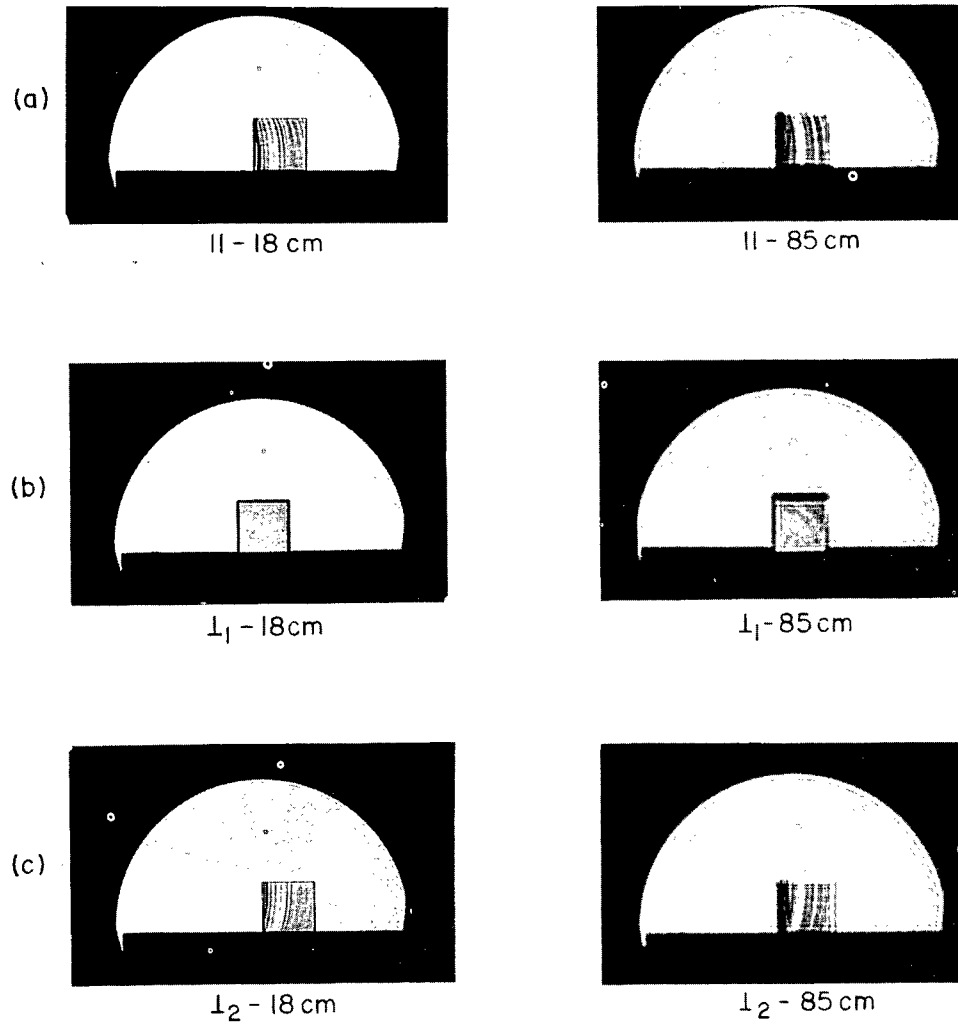


Fig. 16 - Shadowgraphs of Thermal Syndicate 621: (a) parallel to optic axis; (b) first direction perpendicular to optic axis; (c) second direction perpendicular to optic axis

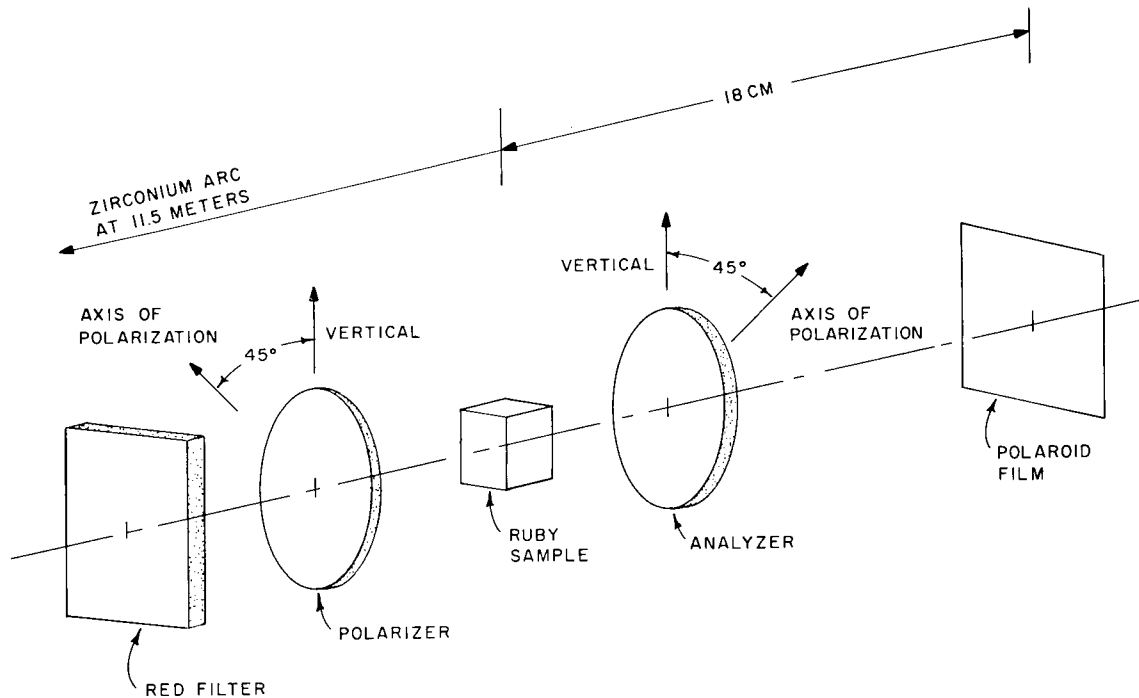


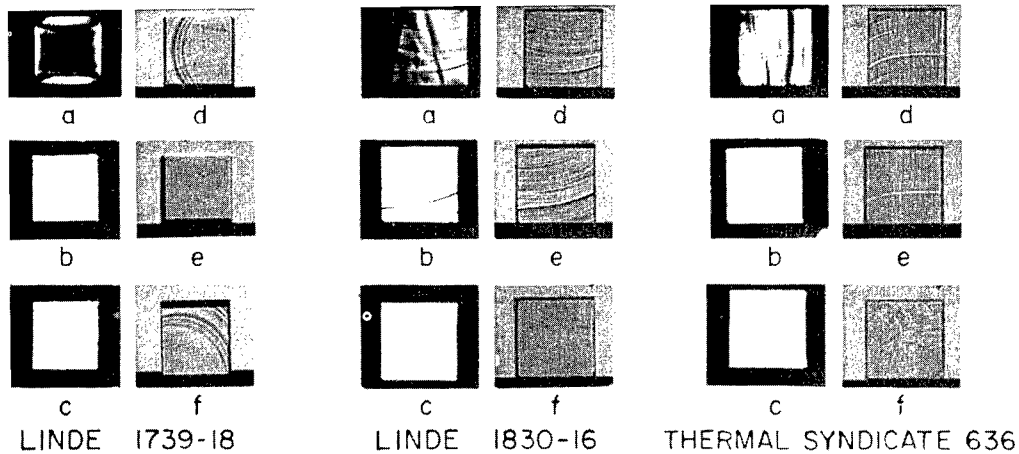
Fig. 17 - Optical system to produce shadowgraphs of samples between crossed polarizers

Linear striae are prominent in all samples except Linde 1963-19. Each of the cubes is relatively free of striae in one direction, although irregularities, somewhat amorphous in appearance, replace the striae in Thermal Syndicate 636. Some of the crystals behave as optical wedges, as evidenced by a lateral displacement of the more distant shadowgraphs. The deviation angles range to nearly a half degree, a deviation much greater than that to be expected from the geometrical nonparallelism of the crystal faces. Such an effect can be produced by a lateral refractive-index gradient of the order of 0.005 to 0.010 per centimeter. Among the sample cubes Linde 1739-18 shows this wedge effect most strongly, but 1830-16 and Thermal Syndicate 621 also cause noticeable deviation. Thermal Syndicate 636 seems to produce a slight deviation. The Airtron crystal causes the largest deviation, about a fifth of which is due to an actual geometrical wedge formed by nonparallel end faces.

Some shadowgraphs have been made with samples between crossed polarizers (Fig. 17), and these are shown along with corresponding shadowgraphs without polarizers (Fig. 18). No attempt has been made to carry this test further, since photo-elastic effects appear to be lost among more gross aberrations.

SMALL-ANGLE SCATTERING

The angular deviations of portions of light beams by the imperfections in the crystals tested (distinct from the whole-beam effects of optical wedges) are all defined here as scattering. The angular deviations introduced by the ruby crystals usually lack axial symmetry, although their characteristics may often be related to features such as striae which are revealed in shadowgraphs. Scattering by inclusions, voids, and dislocations makes some contribution, but evidently a minor one in the crystals observed.



CROSSED POLARIZERS IN PLACE

- a. \parallel , 12-SECOND EXPOSURE
- b. \perp_1 , 6-SECOND EXPOSURE
- c. \perp_2 , 6-SECOND EXPOSURE

SHADOWGRAPHS WITH POLARIZER AND ANALYZER REMOVED

- d. \parallel , 1/5-SECOND EXPOSURE
- e. \perp_1 , 1/5-SECOND EXPOSURE
- f. \perp_2 , 1/5-SECOND EXPOSURE

Fig. 18 - Examination of some ruby samples between crossed polarizers

The small-angle-scattering observation consists mainly in photographing, through a ruby sample, the far-field pattern of an aperture about six millimeters ($1/4$ inch) in diameter. The visible light source is an uncollimated confocal gas laser (λ 6328Å) about 11.5 meters from the aperture (Fig. 19). For convenience, the path was folded by a single 45-degree prism. Again for convenience, exposures were adjusted by a combination of neutral density filters and shutter speeds. A small telescope imaged the source on the film. Ideally there should be no optical elements between light source and aperture, and some of the pictures of the source without a ruby sample demonstrate why. The foreign fringes evidently arise through multiple reflections in the prism and filters. Photographs were made for light incident in three mutually perpendicular directions for each of the finished cubes (Figs. 20-23). Only one direction was possible for the rod (Linde 1963-19) and for the Airtron flux-grown crystal (Fig. 24). Orientations are the same here as for the shadowgraphs, so that direct comparisons may be made. The symbols \parallel , and \perp_1 , and \perp_2 again indicate whether the optic axis of the crystal was parallel or perpendicular to the direction of observation.

Four exposure levels were used. The first, just adequate to record Airy's disk, is arbitrarily designated 1, and the others are greater by factors of 25, 625, and 6250. The peak illuminance of successive diffraction rings varies rapidly near the center. For example, the illuminance for ring one is 60 times less than the peak of Airy's disk, and ring two is 240 times less. Estimates of scattering effects, based on these photographs, must take this into account. The heavier exposures, otherwise, can be quite misleading; they should serve only to describe the nature of the effects. The low exposures are the most significant.

The approximate angular diameters, θ , of the first few "undisturbed" rings are $\theta_1 = 1'10''$; $\theta_2 = 1'56''$; $\theta_3 = 2'40''$; $\theta_4 = 3'24''$; $\theta_5 = 4'06''$.

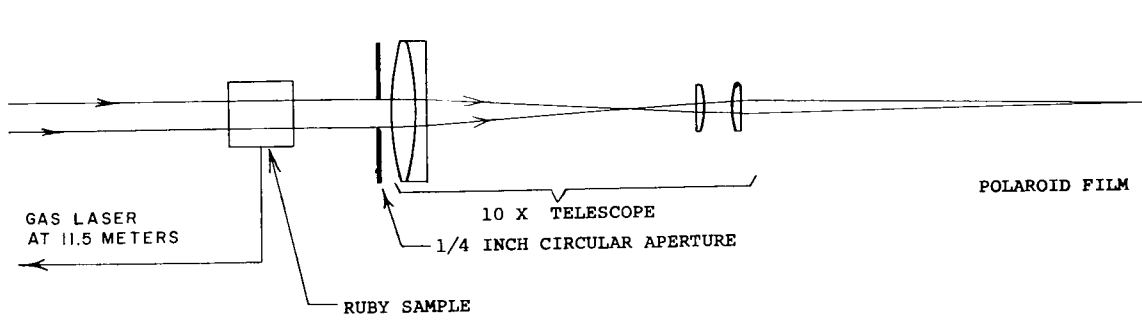


Fig. 19 - Optical system used to observe small-angle scattering

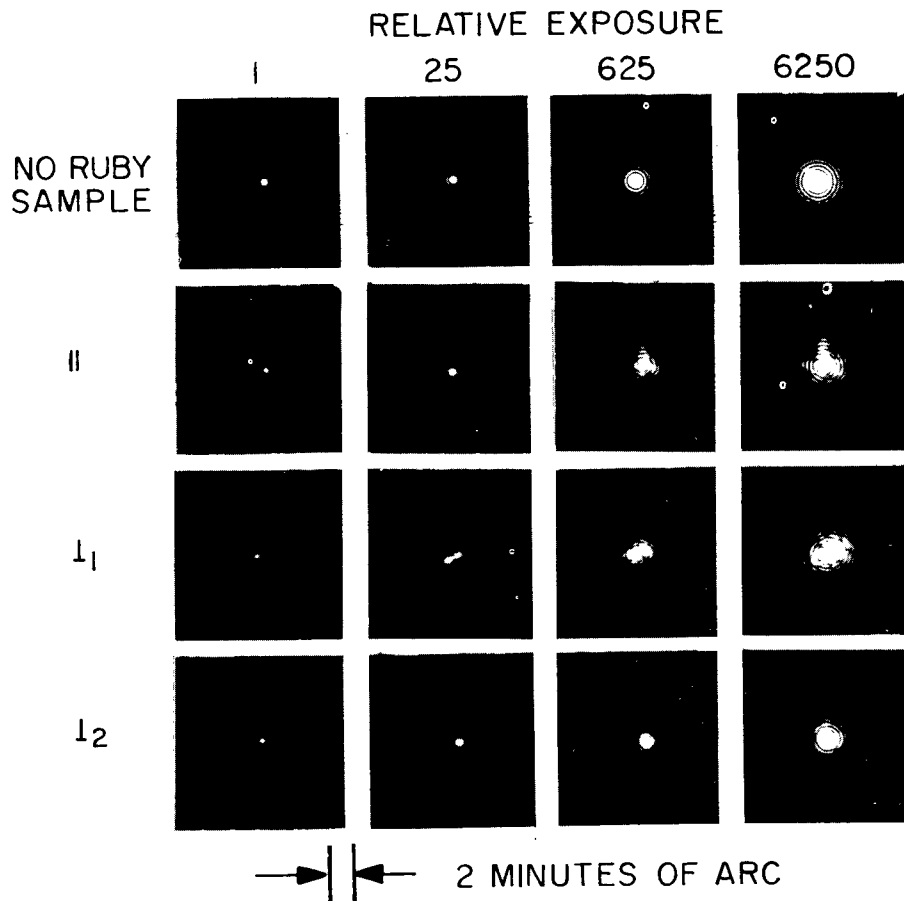


Fig. 20 - Far-field pattern through Linde 1739-18

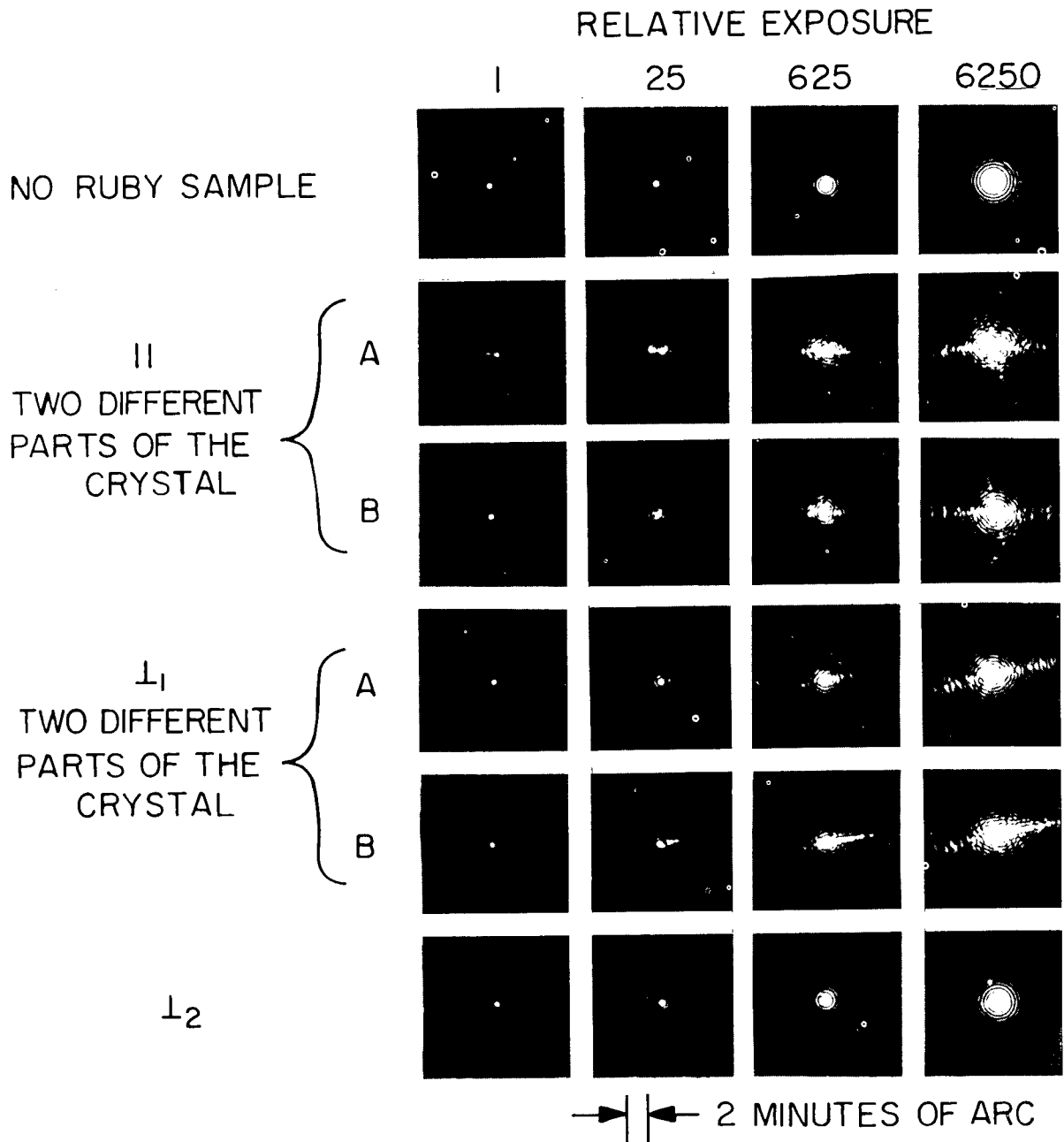


Fig. 21 - Far-field pattern through Linde 1830-16

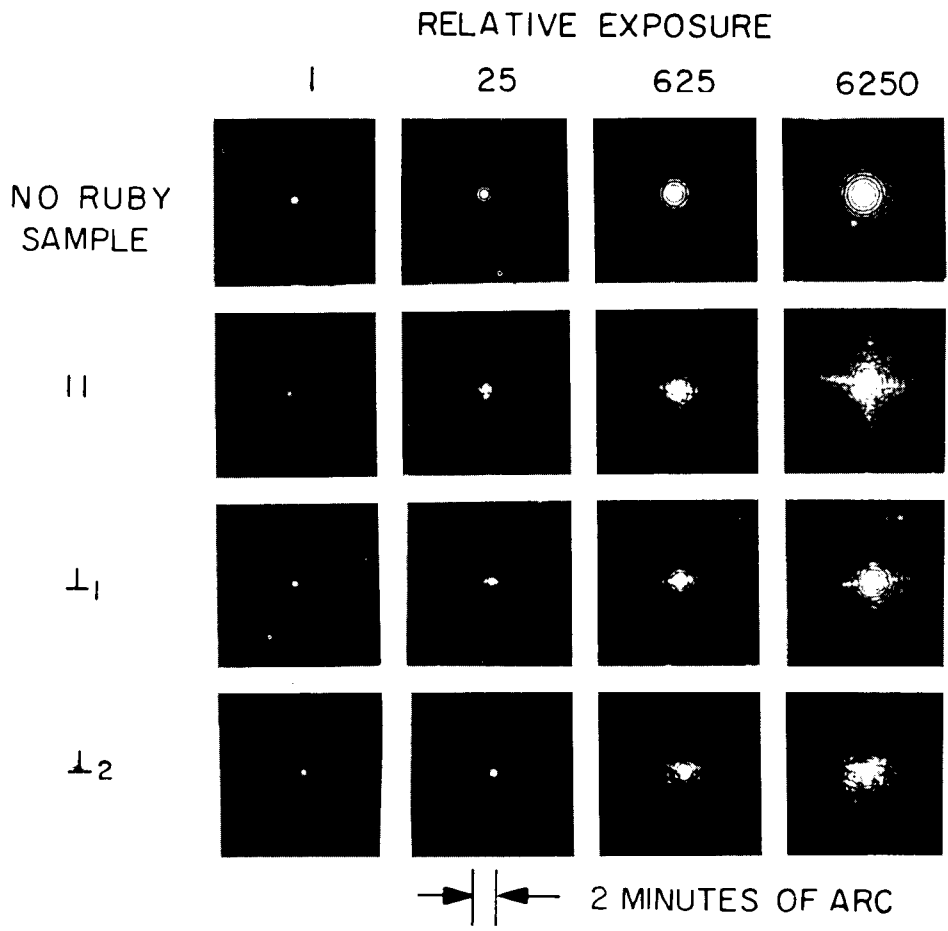


Fig. 22 - Far-field pattern through Thermal Syndicate 636

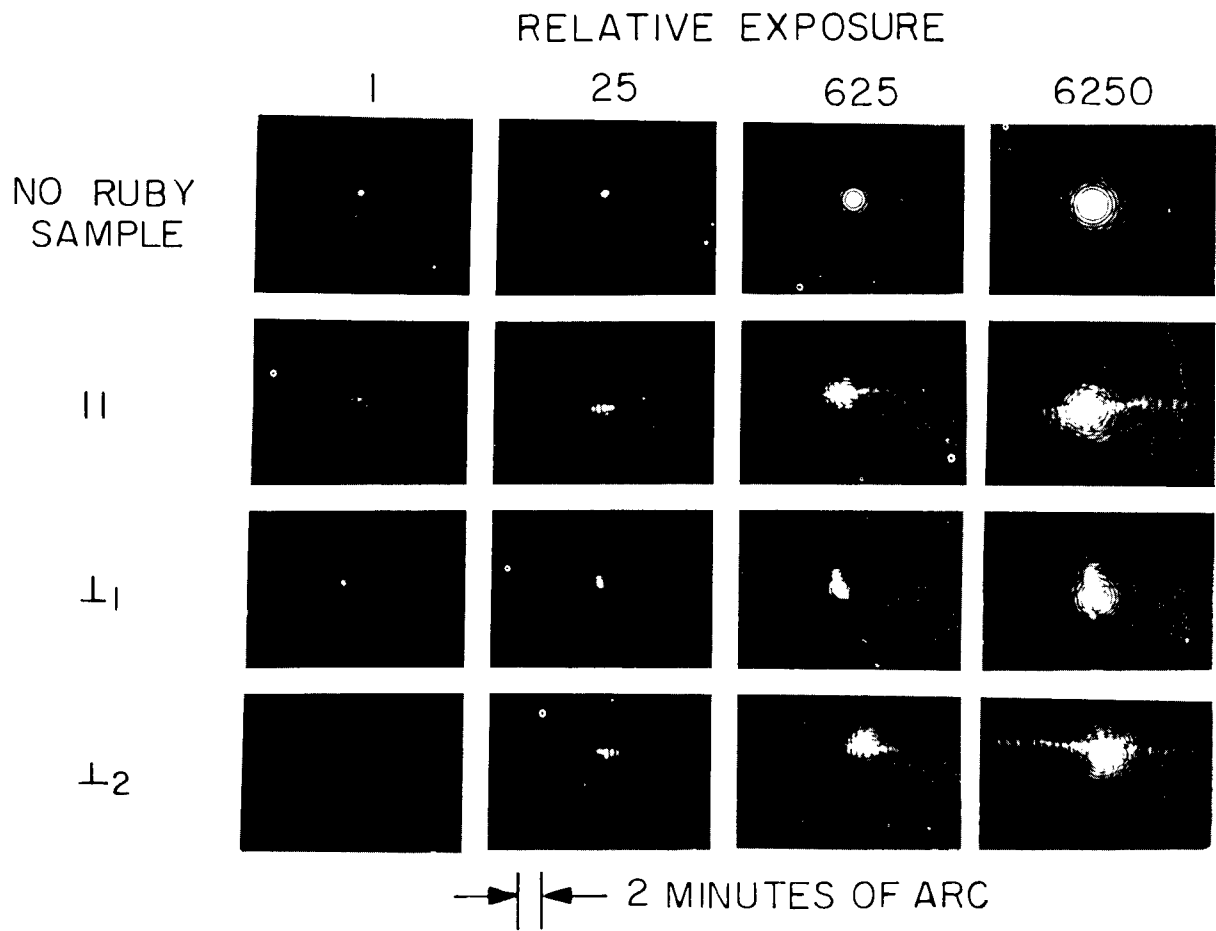


Fig. 23 - Far-field pattern through Thermal Syndicate 621

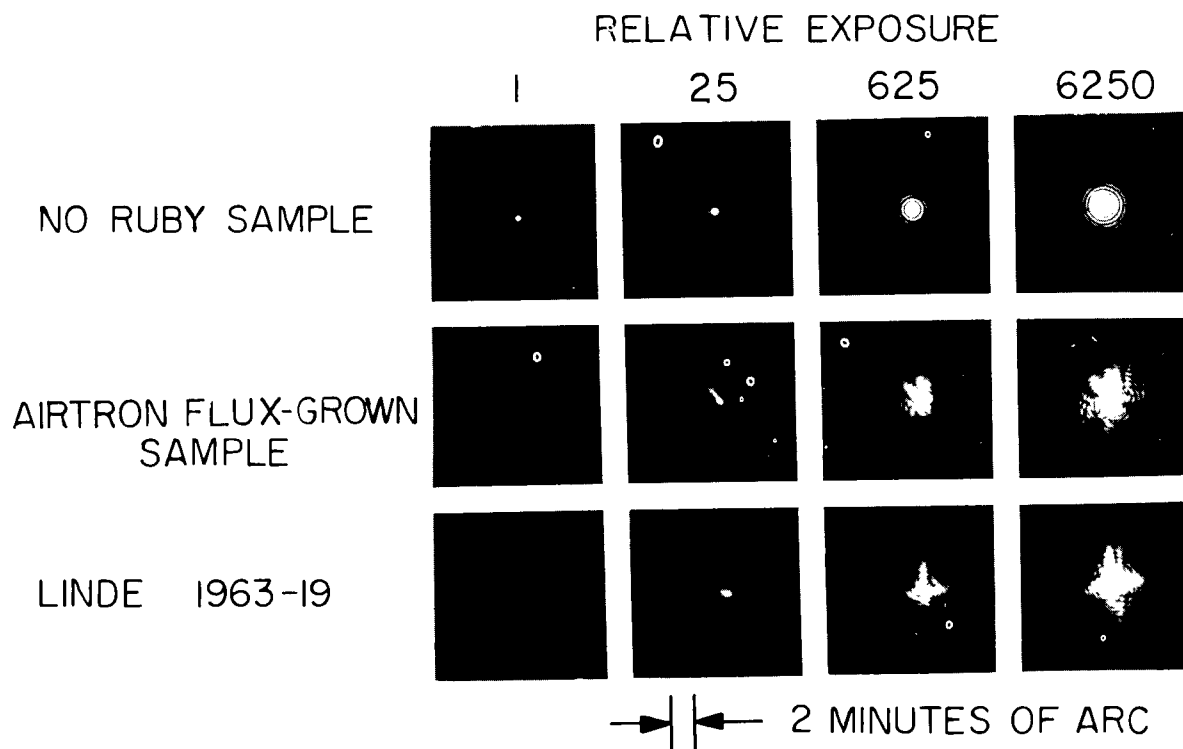


Fig. 24 - FA2-field pattern through airtron flux-grown sample and ruby rod, Linde 1963-19

Table 2
Angular Spread of Airy's Disk by Scattering in
Ruby Crystals

Crystal		⊥ ₁	⊥ ₂
None	0'38"	-	-
Airtron	1'36"	-	-
Linde 1963-19	-	0'48"	-
Linde 1739-18	0'38"	0'38"	1'36"
Linde 1830-16(A)	1'36"	0'38"	0'38"
Linde 1830-16(B)	0'38"	1'36"	-
Thermal Syndicate 636	0'38"	0'38"	0'38"
Thermal Syndicate 621	2'00"	0'48"	1'26"

Some rough angular measurements from the photographs are indicated in Table 2. It is notable that Thermal Syndicate 621 although it is a small cube with short light paths, is quite the poorest of the samples, from the standpoint of scattering. Linde 1963-19, on the other hand, looks very good when the six-cm-path is taken into account. An example of the non-uniformity of some of the materials is Linde 1830-16, in which contiguous regions give different results.

GENERAL OBSERVATIONS

Simple inspection of the ruby samples reveals one serious weakness of present day ruby: non-uniformity of chromium content. Gradations of color are present and, except in the flux-grown crystals, sharp circular bands of color are evidence of abrupt discontinuities in chromium content related to the growth process. Because index of refraction is related to chromium content, these anomalies are assumed to be a major cause of wavefront distortion and small-angle scattering. Chromium content also affects the elastic properties of the crystal and exerts an indirect effect in this way. The location and width of the R_1 fluorescent line also is a function of chromium content.

As index of refraction is a function of the direction of the optic axis, it follows that a perfect crystal from the standpoint of small-angle scattering should have a good optic axis figure. The data here presented show no correlation between optic axis figure and small-angle scattering, e.g., Linde 1830-16 and Thermal Syndicate 636. The influence of other factors on scattering is predominant for the material showing measurable small-angle scattering. With larger samples larger apertures will be possible, and it will be possible to resolve much smaller angular aberrations. The influence of axis uniformity should then be observable.

FUTURE TESTS

It is expected that facilities will soon be available for additional tests that will shed further light on the nature of the inhomogeneities currently present in ruby and which will allow a more sensitive evaluation of improved ruby. Index variations and optical path differences will be investigated with the Twyman-Green interferometer. Strain, chromium concentration variation, and other conditions affecting the fine structure of the energy levels will be investigated by means of high resolution spectroscopy with the samples at liquid helium temperature.